九州大学学術情報リポジトリ
Kyushu University Institutional Repository

Differential activation of proapoptotic molecules between mouse and rat models of distal motor trigeminal denervation

原田, 志織
九州大学大学院歯学府

https://doi.org/10.15017/21764

出版情報：九州大学, 2011, 博士（歯学）, 課程博士
バージョン：
権利関係：(C) 2011 John Wiley & Sons A/S

KYUSHU UNIVERSITY

Differential activation of proapoptotic molecules between mouse and rat models of distal motor trigeminal denervation

Shiori Harada, D.D.S.[1, 2], Satoshi O. Suzuki, M.D., Ph.D.[1], Yoshihiro Seki, D.D.S., Ph.D.[2], Seiji Nakamura, D.D.S., Ph.D.[2], and Toru Iwaki, M.D., Ph.D.[1]

[1]Department of Neuropathology, Graduate School of Medical Sciences, Kyushu University, Fukuoka, Japan

[2]Division of Oral and Maxillofacial Oncology, Faculty of Dental Science, Kyushu University, Fukuoka, Japan.

Corresponding author: Satoshi O. Suzuki, Department of Neuropathology,

Neurological Institute, Graduate School of Medical Sciences, Kyushu University,

3-1-1 Maidashi, Higashi-ku, Fukuoka 812-8582, Japan

Tel.: +81-92-642-5537

Fax: +81-92-642-5540

E-mail: sosuzuki@np.med.kyushu-u.ac.jp

Running title: Trigeminal distal axotomy models

Keywords: Trigeminal motor neuron; axotomy; distal denervation; immunohistochemistry; Noxa

Abstract

[Background] We previously developed a rat trigeminal motor neuron axotomy model involving masseter and temporal muscle resection to study pathological changes of the central nucleus after peripheral nerve injury caused by oral surgery. Because motor neurons are reported to be more vulnerable to axotomy in mice than rats, we compared the degeneration process of the trigeminal motor nucleus in the rat model with a similar mouse model. [Methods] We removed masseter and temporal muscles of adult mice or rats. Animals were sacrificed at 3, 7, 14, 28, 42, and 56 days post-operation, and the trigeminal motor nuclei were histologically analyzed. [Results] Size reduction, but no neuronal loss, was seen in the trigeminal motor nuclei in both mice and rats. Time-dependent Noxa expression, starting at 1 week post-operation (wpo), was seen in the mouse model. By 8 wpo, mice expressed a higher level of Noxa than rats. Additionally, we noted persistent expression of cleaved caspase 3 in mice but not rats. Conversely, apoptosis-inducing factor (AIF), which executes DNA fragmentation in the nucleus, was not translocated to the nucleus in either model. [Conclusions] Our findings indicate differential activation of motor neuron apoptosis pathways after axotomy in mice and rats. Lack of activation of caspase-independent

pathways and distal-end denervation in our model might be related to the survival of motor neurons after axonal injury. These findings could be relevant to future neuroprotective strategies for peripheral nerve injury caused by oral surgeries. (238 words (Limit: 250))

Introduction

It is well established that peripheral nerve axotomy or avulsion causes chronic motor neuron death in the central nervous system, resulting from interruption of target-derived neurotrophic factors (1, 2). Recent investigations have demonstrated that neurons are capable of extending a new growth cone from the axon stump, and that regeneration of peripheral nerves can be attempted by the use of a guidance channel (3). However, without appropriate intervention, most neurons fail to regenerate an axon due to a lack of activation of cell-intrinsic regeneration pathways (4).

Oral surgery often results in a large tissue defect in the head and neck region, although microsurgical reconstruction has facilitated surgical treatment of advanced carcinomas. However, it remains difficult to achieve long-term reconstruction, and the transplanted free muscle flaps become atrophic because of incomplete re-innervation (5–10). Neuronal survival after axotomy is a prerequisite for peripheral nerve regeneration, and is augmented by an array of trophic factors, including neurotrophins, neuropoietic cytokines, insulin-like growth factors, and glial cell line-derived neurotrophic factors (11–15). Neurotrophic factors are supplied to neurons by the distal muscles and Schwann cells. Thus, axotomy causes a cessation of the supply of

neurotrophic factors to neurons, and leads to apoptosis. To achieve an effective functional reconstruction, we posit that it is necessary to regenerate peripheral nerves by combining axonal elongation at the periphery and protection / regeneration of the central nuclei. We previously reported that atrophy of the trigeminal motor nucleus was observed at 8 weeks after resection of the masseter and temporal muscles in adult rats, but no loss of motor neurons was observed. In comparison, it has been reported that approximately 40% of motor neurons disappeared 8 weeks after facial nerve axotomy (16). Moreover, slowly progressive motor neuron death, which took more than a month, occurred after hypoglossal nerve axotomy in the adult mouse, but not in the adult rat. Mice deficient in the p53-inducible Bcl-2 homology domain 3 (BH3)-only protein, Noxa, showed significantly improved survival of axotomized motor neurons. Noxa, located downstream of p53, is a major executor of axotomy-induced motor neuron death in adult mice (17). It is thus hypothesized that the susceptibility of neurons to axotomy is species- and nucleus type-dependent.

A variety of key pro-apoptotic factors have been shown to be involved in caspase-dependent and -independent cell death effector mechanisms. For example, apoptosis-inducing factor (AIF), a flavoprotein localized in the mitochondrial

intermembrane space, has been identified as a caspase-independent apoptotic inducer, which under normal conditions plays a pro-survival role through its redox activity. AIF translocates to the nucleus during apoptosis, and causes peripheral chromatin condensation and large-scale fragmentation of DNA. The nuclear translocation of AIF is implicated in several types of neuronal death and has been shown to play a pivotal role in the apoptotic process (18). In this paper, we generated a mouse model of trigeminal motor neuron axotomy, using resection of the masseter and temporal muscles, to study pathological changes in the trigeminal motor nucleus after peripheral nerve injury in comparison with our previous rat model (19). Using immunohistochemical methods, we also investigated the relevance of the caspase-dependent and -independent apoptotic pathways in these models. We discuss the similarities and differences between our mouse and rat trigeminal motor denervation models, and compare the outcomes with other reported motor denervation models.

Materials and Methods

Animals and surgical procedures

All experimental procedures were conducted in accordance with the Standard Guidelines for Animal Experiments of the Graduate School of Medicine, Kyushu University. Adult C57BL/6 mice (*n* = 18) and adult Sprague-Dawley rats (*n* = 6) were anesthetized by intraperitoneal injection of tribromoethanol (Avertin®, Sigma-Aldrich, St. Louis, MO, USA) (2.5 mg / 10 g weight), and the left masseter and temporal muscles were completely removed. The wounds were closed with α-cyanoacrylate surgical glue (Aron-Alpha®, Toagosei, Tokyo, Japan). The behaviors of the animals were observed postoperatively until they were confirmed as being capable of feeding.

Tissue preparation and immunohistochemistry

Animals (three for each time point) were perfused with 4% paraformaldehyde in phosphate-buffered saline (PBS; pH 7.4) at 3, 7, 14, 28, 42, and 56 days post-operation (dpo) under deep anesthesia, and brains were post-fixed in the same fixative for 1 day at 4 °C. Brains were then cryoprotected in PBS containing 30% sucrose before being sectioned. The brain stem tissue containing the trigeminal motor nucleus was dissected

out, embedded in OCT compound (Tissue-Tek, Torrance, CA, USA) and snap-frozen in 2-methylbutane at -80 °C, and stored at -80 °C until use. Cryosections (18 μm thickness) were cut to cover the entire volume of the trigeminal motor nucleus. Some of the tissues were processed into 5 mm-thick paraffin sections. The sections were routinely stained with hematoxylin and eosin. Immunohistochemistry was performed using the streptavidin–biotin complex method.

The following antibodies were used: rabbit anti-Noxa polyclonal antibody (1:1000 dilution; ab36833, Abcam, Cambridge, UK); rabbit anti-AIF polyclonal antibody (1:50 dilution; Cell Signaling Technology, Danvers, MA, USA); and rabbit anti-cleaved caspase 3 polyclonal antibody (1:200 dilution; Cell Signaling Technology); mouse anti-synaptophysin monoclonal antibody (1:100 dilution; M0776, DAKO). The rabbit anti-Noxa polyclonal antibody was raised against a synthetic peptide corresponding to 17 amino acids at the amino terminus of mouse Noxa and cross-reacts with rat Noxa due to sequence homology. After washing twice with Tris–HCl (50 mM; pH 7.6), the sections were pre-treated with 0.3% H_2O_2 in absolute methanol for 30 min at room temperature to block endogenous peroxidase activity. Tissue sections were subjected to heat-induced epitope retrieval by autoclaving them in a 0.01M citrate

buffer (pH 6.0) at 121 °C for 10 min. After rinsing twice with Tris–HCl containing 0.1% Triton X-100 and once with Tris–HCl, the sections were incubated overnight with primary antibodies diluted in PBS containing 5% normal goat serum or 5% milk at 4 °C. The signal was developed in 0.2 mg/ml diaminobenzidine tetrahydrochloride/Tris–HCl (pH 7.6) containing 0.003% H_2O_2. Sections were lightly counterstained with hematoxylin, dehydrated in an ethanol gradient, and coverslipped.

Immunostaining with the mouse monoclonal antibodies were performed using Histofine MOUSESTAIN KIT (Nichirei, Japan).

Quantitative analyses and statistics

The outline of the trigeminal motor nucleus was traced to the sectioning level at which the nucleus size is at its maximum, and the enclosed area was painted out in black using imaging software (Photoshop 7.0; Adobe Systems, San Jose, CA, USA). The area of the nucleus was measured by IMAGE J software (NIH imaging) (n = 12). Moreover, the number of trigeminal motor neurons was counted at the same sectioning level (n = 12). Results are expressed as the ratio of values obtained in the injured or contralateral (non-injured) nuclei to those in the non-operated control group. All data

are presented as the mean ± SEM and are analyzed using one-way ANOVA with a *post hoc* Scheffe's test. Statistical significance was established at a level of $P < 0.05$.

Results

Axotomized trigeminal motor nucleus atrophies with glial reaction

At each post-operative time point, we cut serial sections of the brain stem to cover the entire volume of the trigeminal motor nucleus, and compared the pathologic changes between the ipsilateral and contralateral sides in slices where trigeminal motor nucleus size was at its maximum. From 2–6 weeks post-operation (wpo), the number of trigeminal motor neurons and the size of the trigeminal motor nucleus were not significantly different between the denervated and contralateral sides (Fig. 1 A–H). At 8 wpo, the size of the ipsilateral trigeminal motor nucleus was significantly reduced (~25% reduction) (Fig. 1 A–D, J). The number of injured neurons in the trigeminal motor nucleus in our mouse model was unaltered (Fig. 1 I). In addition, degenerative changes, such as central chromatolysis and apoptosis, were not obviously apparent in the ipsilateral trigeminal motor nucleus, even at high magnification. On the other hand, in the affected nuclei, immunohistochemistry for synaptophysin showed decreased synaptic staining along the surface of neuronal somata (Fig. 1 K, L), as we previously observed in the rat model (19), suggesting that the size reduction of the nuclei was mainly caused by degeneration of neurites and synapses in the nuclei.

To study glial reactions in response to axotomy, we performed immunohistochemistry for Iba-1 and GFAP in the trigeminal motor nuclei. The number of Iba1-positive microglia was gradually increased in the ipsilateral trigeminal motor nucleus. Maximum Iba1-immunoreactivity was observed at 3 dpo (Fig. 2). Iba1-positive microglia exhibited activated morphology, with processes extending towards the perikarya of the motor neurons. Immunohistochemistry for GFAP revealed astrocytic reactions in the trigeminal motor nucleus on the lesioned side. GFAP expression was observed at 3 days after the removal of the muscles and, over time, astrocytes in and around the trigeminal motor nucleus on the lesioned side underwent typical reactive changes, including hypertrophy and multipolar process extension. GFAP expression peaked at 4 wpo (Fig. 2).

Differential Noxa expression between mice and rats in response to nerve injury.

High Noxa activity in mice is thought to be responsible for the slowly (> 1 month) progressive motor neuron death that occurs after hypoglossal axotomy in adult mice but not rats (17). Consistent with this hypothesis, Noxa expression was observed within 1 wpo in our mouse trigeminal motor neuron axotomy model and gradually

increased in a time dependent manner, peaking at 8 wpo (Fig. 3A). In comparison, Noxa expression was not observed in axotomized trigeminal motor neurons in the rat model throughout the postoperative period up to 8 wpo (Fig. 3B).

The caspase-dependent apoptosis pathway, but not caspase-independent pathway, was activated in the axotomized trigeminal motor nucleus.

Expression of cleaved caspase 3 in mice was observed at 1 wpo, and continued to the same level towards 8 wpo. In contrast, AIF was expressed from 2–6 wpo, but not at 8 wpo (Fig. 4). AIF was localized to perikarya of the motor neurons and neuropil, but did not redistribute to the nuclei.

Discussion

Noxa expression was observed in our mouse trigeminal motor neuron axotomy model, but not in the equivalent rat model. Furthermore, expression of cleaved caspase 3 in mice was observed at 1 wpo, and it continued at the same level towards 8 wpo. Noxa is induced by p53 and plays a role in activating the caspase-dependent apoptotic pathway. It has been reported that mouse motor neurons are more susceptible to axotomy than are those of rats, and that motor neuron loss after hypoglossal axotomy is seen only in mice (17). This difference has been attributed to a species-specific difference in the expression level of Noxa. Because Noxa is expressed in injured motor neurons in mice but not in rats, it is implicated in determining the fate of injured motor neurons (17). Our results confirm previous observations of species-specific Noxa expression patterns, and suggest that the apoptotic pathway is initiated after denervation in the mouse axotomy model. Nevertheless, the mouse model showed only late, moderate atrophy of the trigeminal motor nucleus, with no obvious neuronal loss as we previously observed in the rat model (19).

There are various possible explanations for these results. In our axotomy models, denervation was designed to occur at the most distal end of the trigeminal

motor nerve fibers around which they innervate the target muscles, whereas in the previous hypoglossal and facial nerve axotomy models a more proximal axotomy was performed. Specifically, in our model, the trigeminal motor axons were cut at the levels of the deep temporal and masseteric branches of the mandibular nerve. A distal lesion should result in the preservation of a greater proportion of the central axons, together with a larger number of the Schwann cells that cover them and serve as a source of protective factors for the injured motor neurons.

In the caspase-dependent apoptotic pathway, caspase-activated deoxyribonuclease (CAD) has been identified as the terminal executor of chromosomal DNA degradation. Activated caspase-3 releases CAD from inhibitor of CAD (ICAD) by cleaving ICAD, allowing CAD to enter the nucleus and degrade chromosomal DNA (22). Tanaka et al. reported that induction of global ischemia in animals that had been subjected to ischemic preconditioning in advance triggered activation of caspase-3, but failed to increase nuclear CAD or cause DNA fragmentation in the CA1 neurons (23). The same group also revealed that preconditioning preserved the integrity of the mitochondrial membrane, blocking the release of Smac/DIABLO, an enhancer of caspase-3 activity, and thereby enabled CA1 neurons to survive (24). An ultrastructural

study also showed that expression of activated-caspase-3 preceded chromatin condensation in dopaminergic neurons of a human Parkinson's disease tissue, but the expression disappeared in the neurons once showing typical morphologic features of apoptosis (25). These studies indicate that activation of caspase-3 can initiate the apoptotic process, but it does not necessarily coincide with DNA degradation, nor does always mean its expression destines a cell to die. Since Noxa works upstream of caspase-3 activation, if the effector of apoptosis located downstream of caspase-3 activation is blocked, motor neurons could evade apoptosis even when they express both Noxa and cleaved caspase-3. In the denervation at the extreme end of the axon used in our model, which would add slowly affecting insults to the motor neurons, the integrity of mitochondria membrane may be preserved as in the ischemic preconditioning.

AIF-dependent cell death, one of the caspase-independent pathways of programmed cell death, was originally reported to control early morphogenesis (20). It was later also shown to play a role in pathological cell death (18). AIF is an apoptotic effector protein that induces chromatin condensation and large-scale (50 kbp) DNA fragmentation (21) following translocation to the nucleus. In our model, AIF was

upregulated temporarily in motor neurons (between 2–6 wpo), but its expression was restricted to the perikarya and neuropil, and at no time point did it redistribute to the nucleus. This lack of activation of caspase-independent pathways may also underlie the enhanced survival of motor neurons observed after distal axonal injury. Additionally, it is possible that motor neurons of different motor nuclei have variable vulnerability to axonal injury.

The pathological findings in our present model could specifically represent the consequences of distal axonal injury and may closely mimic the practical conditions of human oral surgery. If axotomized trigeminal motor neurons in humans also evade apoptosis after oral surgery, protection of the central nucleus would have clinical significance in functional regeneration of innervation. Further evidence from human case studies as well as investigation of the apoptotic process downstream of caspase-3 activation in the axotomized neurons is required to confirm the pathological effects of target muscle removal on the central nuclei.

References

1 Imamoto K. Fine structural changes in the trigeminal motor nucleus following neurotomy of the third division of the trigeminal nerve. Arch Histol Jpn 1973; 35: 175–94.

2 Bilbao F, Dubois-Dauphin M. Time course of axotomy induced apoptotic cell death in facial motoneurons of neonatal wild type and bcl-2 transgenic mice. Neurosci 1996; 71: 1111–9.

3 Piquilloud G, Christen T, Pfister LA, Gander B, Papaloïzos MY. Variations in glial cell line-derived neurotrophic factor release from biodegradable nerve conduits modify the rate of functional motor recovery after rat primary nerve repairs. Eur J Neurosci 2007; 26: 1109–17.

4 Liu BP, Cafferty WB, Budel SO, Strittmatter SM. Extracellular regulators of axonal growth in the adult central nervous system. Philos Trans R Soc Lond B Biol Sci 2006; 361: 1593-610.

5 Hara I, Gellrich NC, Duker J, et al. Swallowing and speech function after intraoral soft tissue reconstruction with lateral upper arm free flap and radial forearm free flap. Br J Oral Maxillofac Surg 2003; 41: 161–9.

6 Michiwaki Y, Schmelzeisen R, Hacki T, Michi K. Articulatory function in glossectomized patients with immediate reconstruction using a free jejunum flap. J Craniomaxillofac Surg 1992; 20: 203–10.

7 Nicoletti G, Soutar DS, Jackson MS, Wrench AA, Robertson G. Chewing and swallowing after surgical treatment for oral cancer: functional evaluation in 196 selected cases. Plast Reconstr Surg 2004; 114: 329–38.

8 Yamamoto Y, Sugihara T, Furuta Y, Fukuda S. Functional reconstruction of the tongue and deglutition muscles following extensive resection of tongue cancer. Plast Reconstr Surg 1998; 102: 993–8.

9 Crumley RL. Mechanisms of synkinesis. Laryngoscope 1979; 89: 1847–54.

10 Araki K, Shiotani A, Watabe K, Saito K, Moro K, Ogawa K. Adenoviral GDNF gene transfer enhances neurofunctional recovery after recurrent laryngeal nerve injury. Gene Ther 2006; 13: 296–303.

11 Houenou LJ, Oppenheim RW, Li L, Lo AC, Prevette D. Regulation of spinal motoneuron survival by GDNF during development and following injury. Cell Tissue Res 1996; 286: 219–23.

12 Graeber MB, Raivich G, Kreutzberg GW. Increase of transferrin receptors and iron uptake in regenerating motor neurons. J Neurosci Res 1989; 23: 342–5.

13 Haas CA, Donath C, Kreutzberg GW. Differential expression of immediate early genes after transection of the facial nerve. Neuroscience 1993; 53: 91–9.

14 Sendtner M, Kreutzberg GW, Thoenen H. Ciliary neurotrophic factor prevents the degeneration of motor neurons after axotomy. Nature 1990; 345: 440–1.

15 Streit WJ, Kreutzberg GW. Response of endogenous glial cells to motor neuron degeneration induced by toxic ricin. J Comp Neurol 1988; 268: 248–63.

16 Dauer DJ, Huang Z, Ha GK, Kim J, Khosrowzadeh D, Petitto JM. Age and facial nerve axotomy-induced T cell trafficking: Relation to microglial

and motor neuron status. Brain Behav Immun 2011; 25: 77-82.

17 Kiryu-Seo S, Hirayama T, Kato R, Kiyama H. Noxa is a critical mediator of p53-dependent motor neuron death after nerve injury in adult mouse. J Neurosci 2005; 25: 1442–7.

18 Murakami Y, Ikeda Y, Yonemitsu Y, et al. Inhibition of Nuclear Translocation of Apoptosis-Inducing Factor Is an Essential Mechanism of the Neuroprotective

Activity of Pigment Epithelium-Derived Factor in a Rat Model of Retinal Degeneration. Am J Pathol 2008; 173:1326−38.

19 Seki Y, Suzuki SO, Nakamura S, Iwaki T. Degenerative and protective reactions of the rat trigeminal motor nucleus after removal of the masseter and temporal muscles. J Oral Pathol Med 2009; 38: 777–84.

20 Joza N, Susin SA, Daugas E, et al. Essential role of the mitochondrial apoptosis-inducing factor in programmed cell death. Nature 2001; 410: 549−54.

21 Daugas E, Susin SA, Zamzami N, et al. Mitochondrio-nuclear translocation of AIF in apoptosis and necrosis. J FASEB 2000; 14: 729−39.

22 Enari M, Sakahira, S, Yokoyama H, et al. A caspase-activated DNase that degrades DNA during apoptosis, and its inhibitor ICAD. Nature 1998; 391: 43–50

23 Tanaka H, Yokota H, Teresa J, et al. Ischemic Preconditioning: Neuronal survival in the face of caspase-3 activation. J Neurosci 2004; 24: 2750 –59

24 Miyawaki T, Mashiko T, Ofengeim D, et al. Ischemic preconditioning blocks BAD translocation, Bcl-xL cleavage, and large channel activity in mitochondria of postischemic hippocampal neurons. Proc Natl Acad Sci USA 2008; 105: 4892-97

25 Andreas H, Stephane H, Patrick PM, et al. Caspase-3: A vulnerability factor and final effector in apoptotic death of dopaminergic neurons in Parkinson's disease. PNAS 2000; 97: 2875–80

Figure legends

Figure 1. Time-course of histological changes in the mouse trigeminal motor nucleus. Representative images of H&E-stained paraffin sections of mouse trigeminal nucleus at 2 (A, E), 4 (B, F), 6 (C, G), and 8 (D, H) weeks after removal of the left masseter and temporal muscles. Ipsilateral (A, B, C, D) and contralateral (E, F, G, H) sides are shown. Size reduction of the nucleus was seen in the ipsilateral side, but neuronal loss is not evident. Quantitative analysis (I, J) shows that the injured trigeminal motor nucleus is reduced in size on the ipsilateral side at 8 weeks, but without significant change in the number of motor neurons. Data are mean ± SEM ($n = 3$; $^*P < 0.05$). Immunohistochemistry for synaptophysin (K, L) in paraffin sections. Photomicrographs show the trigeminal motor nucleus on the ipsilateral side (K) and the contralateral side (L) at 8 weeks. Scale bars: 100 μ m.

Figure 2. Immunohistochemistry for Iba-1 (A) and GFAP (B, C) in frozen sections. Photomicrographs show the trigeminal motor nucleus on the ipsilateral side at 3 days (A, B) or 4 weeks (C) post-operation.

Figure 3. Immunohistochemistry for Noxa in frozen sections. A, Photomicrographs show the trigeminal motor nucleus on the ipsilateral side at 1 (a), 2 (b), 4 (c) or 6 (d) weeks post-operation. Expression of Noxa was evident at 1 week and increased time-dependently. Scale bars: 30μm. B, By 8 weeks post-operation, the mice (a, b) expressed a higher level of Noxa than the rats (c, d). Key: ope, operated side; cont, contralateral side. Scale bars: 500 μm (a, c), 30 μm (b, d)

Figure 4. Immunohistochemistry for cleaved caspase 3 and apoptosis-inducing factor (AIF) in frozen sections. Photomicrographs show the mouse trigeminal motor nucleus on the ipsilateral side at 2 (A, E), 4 (B, F), 6 (C, G) or 8 (D, H) weeks after axotomy of trigeminal motor neurons. Cleaved caspase 3 immunoreactivity (A, B, C, D) was seen at 2–8 weeks post-operation. AIF immunoreactivity (E, F, G, H) was observed within 2–6 weeks, and localized to the perikarya and neuropil. Scale bars: 30 μm.

Figure 1.

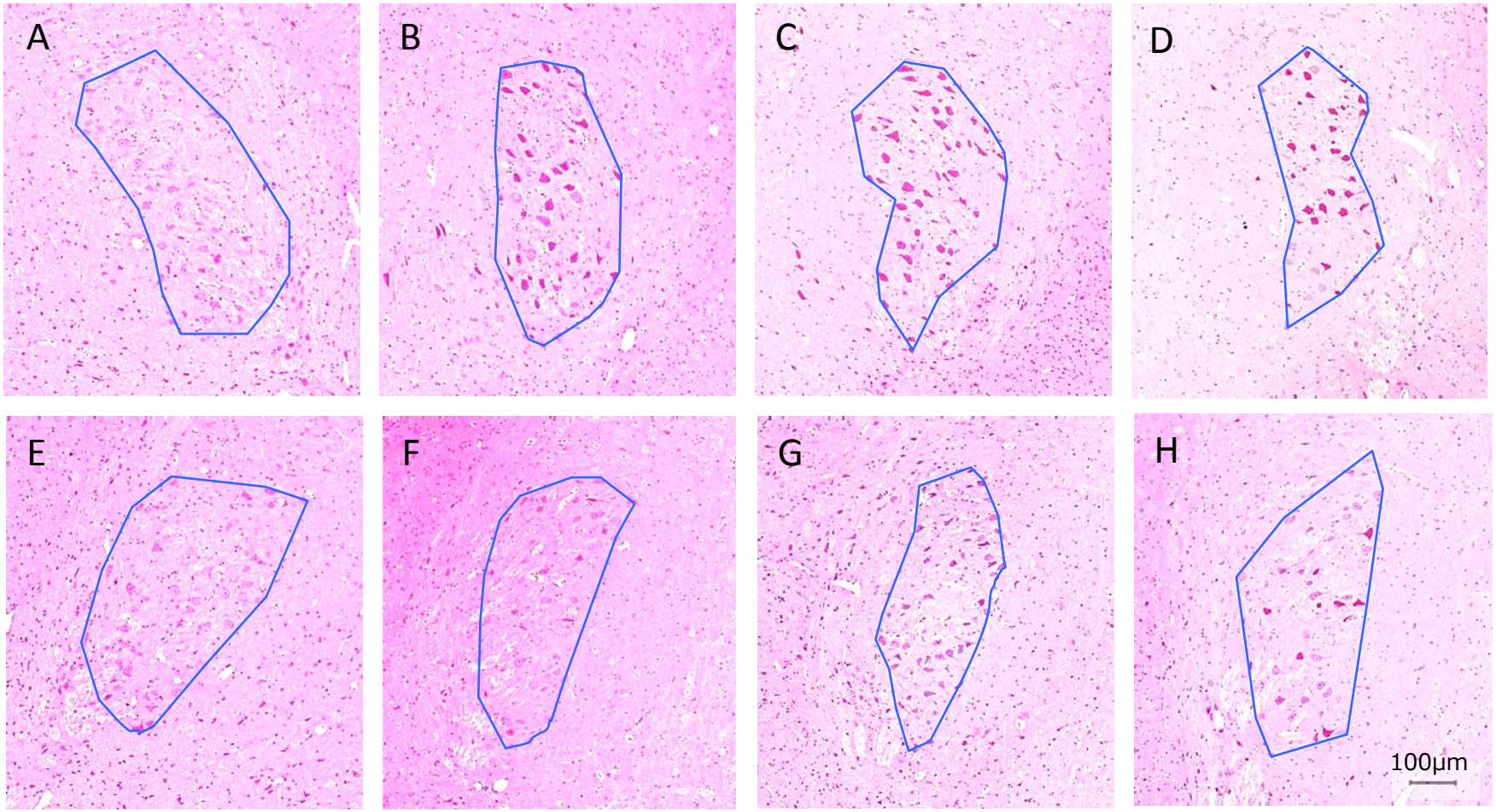

I

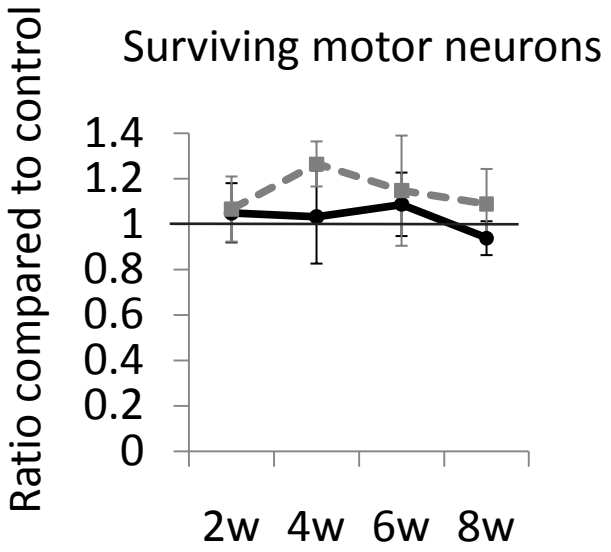
Surviving motor neurons
Ratio compared to control
1.4
1.2
1
0.8
0.6
0.4
0.2
0
2w
4w
6w
8w

J

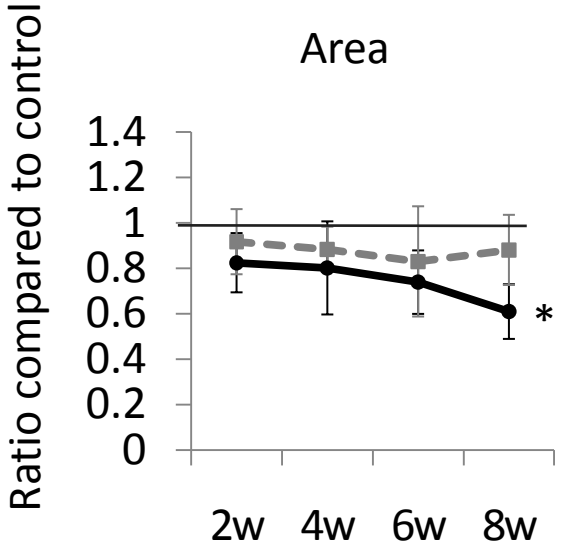
Area
Ratio compared to control
1.4
1.2
1
0.8
0.6
0.4
0.2
0
*
2w
4w
6w
8w

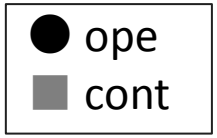
ope
cont

* P < 0.05

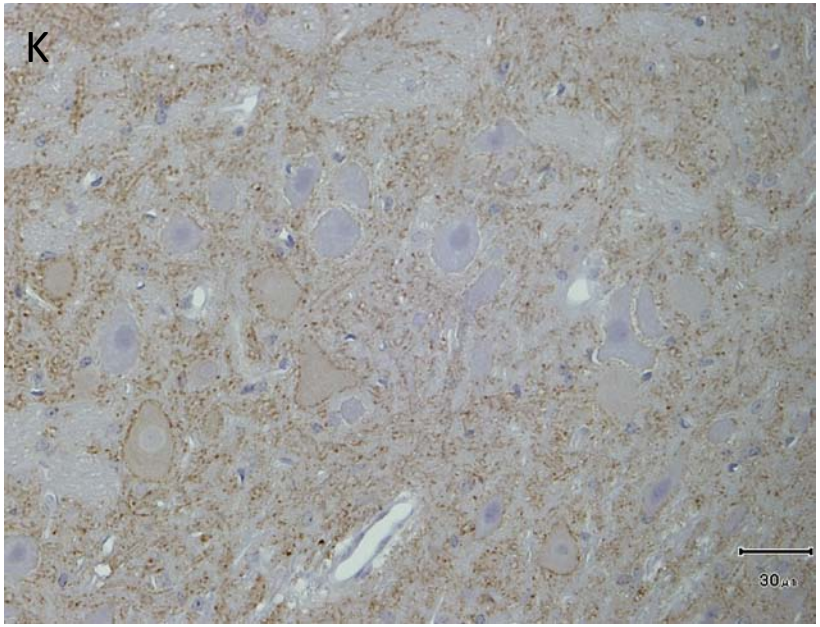
K
30 μm

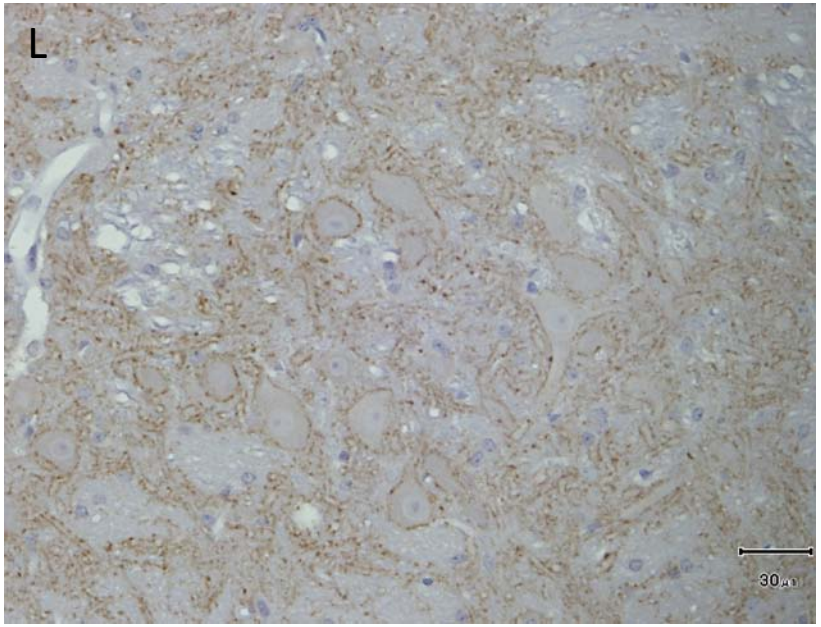
L
30 μm

Figure 2.

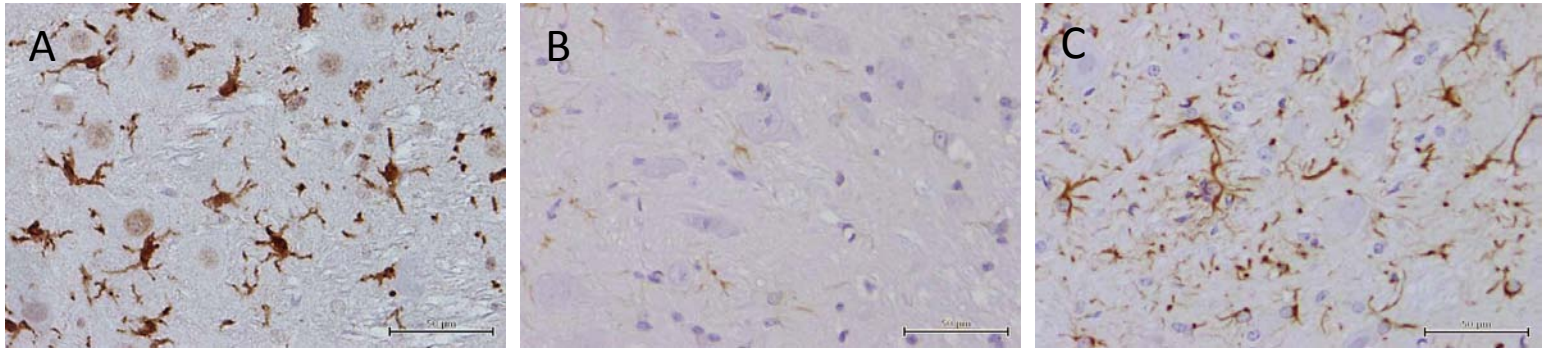

Figure 3.

A

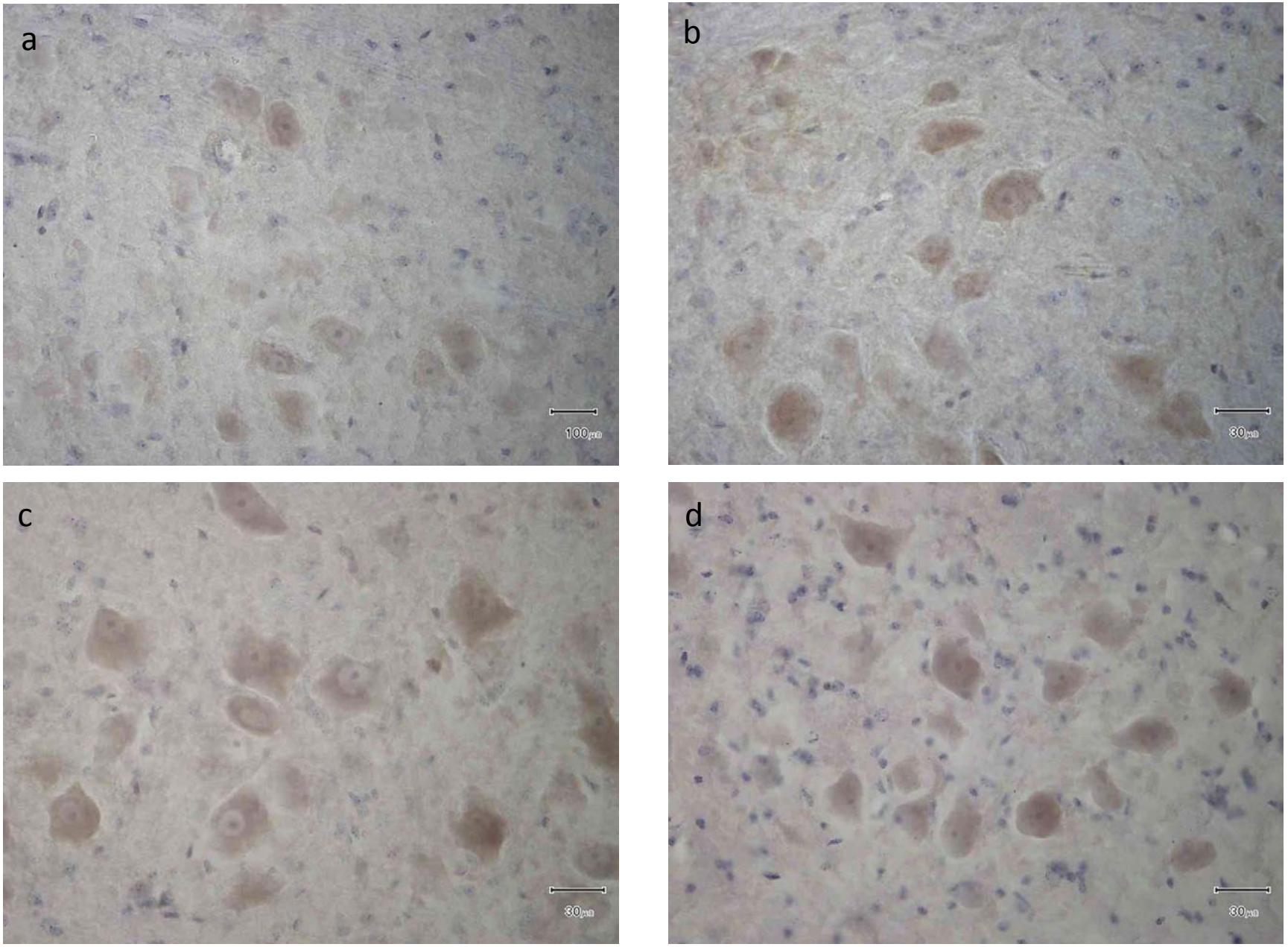

B

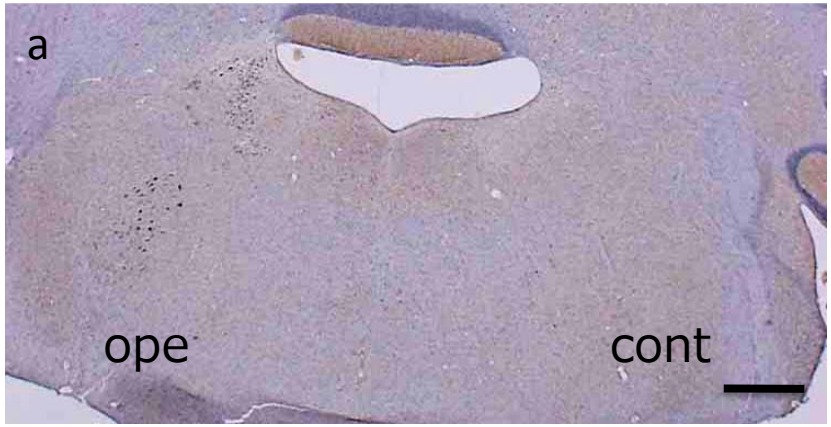

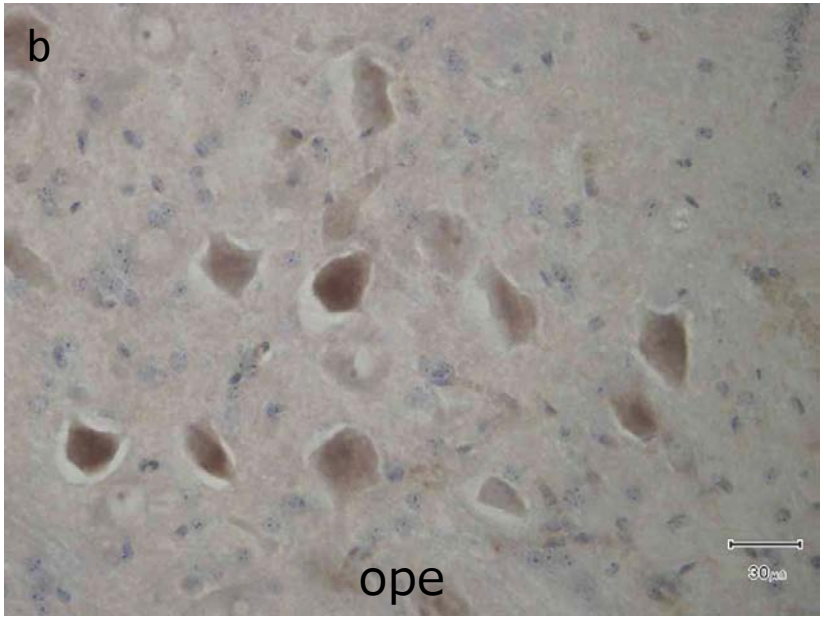

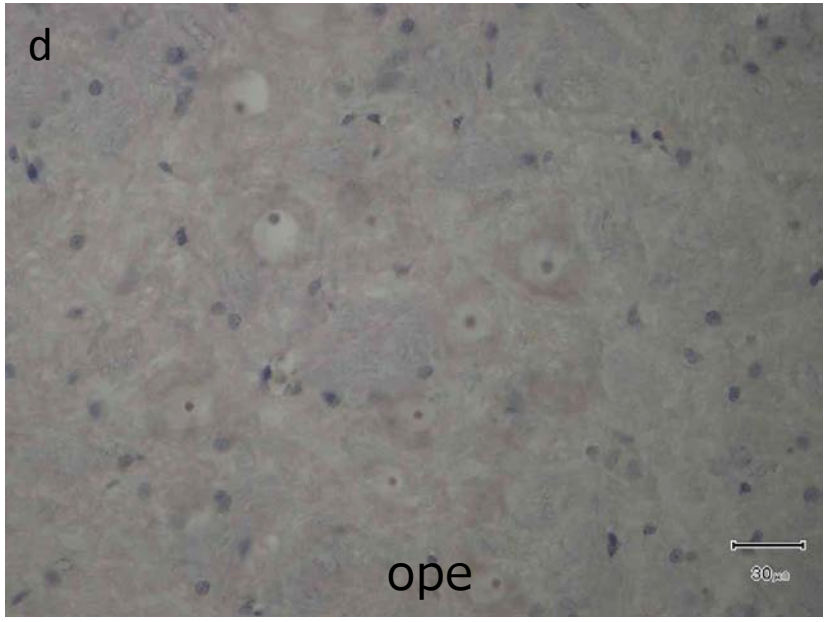

Figure 4.